

# Oxidation of Methanol by $\text{FeO}^{2+}$ in Water: DFT Calculations in the Gas Phase and Ab Initio MD Simulations in Water Solution

Manuel J. Louwerse,\* Peter Vassilev, and Evert Jan Baerends\*

Theoretical Chemistry, Vrije Universiteit Amsterdam, De Boelelaan 1083, 1081 HV Amsterdam, The Netherlands

Received: July 26, 2007; In Final Form: October 24, 2007

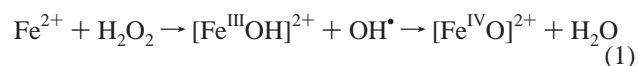
We investigate the mechanism of methanol oxidation to formaldehyde by ironoxido ( $[\text{Fe}^{\text{IV}}\text{O}]^{2+}$ ), the alleged active intermediate in the Fenton reaction. The most likely reaction mechanisms are explored with density functional theory (DFT) calculations on microsolvated clusters in the gas phase and, for a selected set of mechanisms, with constrained Car-Parrinello molecular dynamics (CPMD) simulations in water solution. Helmholtz free energy differences are calculated using thermodynamic integration in a simulation box with 31 water molecules at 300 K. The mechanism of the reaction is investigated with an emphasis on whether  $\text{FeO}^{2+}$  attacks methanol at a C–H bond or at the O–H bond. We conclude that the most likely mechanism is attack by the oxido oxygen at the C–H bond (“direct CH mechanism”). We calculate an upper bound for the reaction Helmholtz free energy barrier in solution of 50 kJ/mol for the C–H hydrogen transfer, after which transfer of the O–H hydrogen proceeds spontaneously. An alternative mechanism, starting with coordination of methanol directly to Fe (“coordination OH mechanism”), cannot be ruled out, as it involves a reaction Helmholtz free energy barrier in solution of  $44 \pm 10$  kJ/mol. However, this coordination mechanism has the disadvantage of requiring a prior ligand substitution reaction, to replace a water ligand by methanol. Because of the strong acidity of  $[\text{FeO}(\text{H}_2\text{O})_5]^{2+}$ , we also investigate the effect of deprotonation of a first-shell water molecule. However, this is found to increase the barriers for all mechanisms.

## 1. Introduction

As early as in 1876, H. J. H. Fenton discovered the strongly accelerating effect of  $\text{Fe}^{2+}$  ions on oxidation by hydrogen peroxide,<sup>1</sup> which later turned out to be a catalytic process. Since then, this mixture of hydrogen peroxide and ferrous ions in water has become known as Fenton’s reagent, and it can efficiently oxidize most organic compounds. Nowadays, Fenton’s reagent is used in a broad range of industrial applications, like the oxidation of wastewater,<sup>2</sup> the hydroxylation of aromatic substrates,<sup>3</sup> and many other reactions.

Despite this wide variety of applications, the mechanism of the Fenton reaction remains controversial.<sup>4–8</sup> Experimentally, it has been very difficult to determine whether free  $\text{OH}^\bullet$  radicals are the exclusive intermediates in the reaction, whether they play an important but non-exclusive role, or whether the organic substrate is attacked by another intermediate altogether. The prime candidate for an alternative intermediate is the  $\text{FeO}^{2+}$  ion.<sup>9</sup> Using both calculations on the microsolvated system in the gas phase and Car-Parrinello molecular dynamics (CPMD) simulations of  $\text{Fe}^{2+} + \text{H}_2\text{O}_2$  in water solution (periodic systems with 31 water molecules per unit cell), Ensing et al.<sup>10–13</sup> have provided evidence that the most important active intermediate is the  $\text{FeO}^{2+}$  species. It is commonly assumed (and confirmed in these simulations) that the first step of the reaction is the homolytic dissociation of the O–O bond of a coordinated  $\text{H}_2\text{O}_2$ , producing an  $\text{OH}^-$  ligand (taking one electron from iron) and an OH radical. However, as Ensing et al. have emphasized, the formation of a free OH radical is energetically unfavorable: the bond dissociation energy of  $\text{H}_2\text{O}_2$  of ca. 250 kJ/mol is only

partly compensated by the stronger bonding of the OH left behind to the Fe center (formally  $\text{OH}^-$  to  $\text{Fe}^{3+}$ ), which is only ca. 160 kJ/mol stronger than the coordination of  $\text{H}_2\text{O}_2$  to  $\text{Fe}^{2+}$ .<sup>12</sup> Instead, the OH radical immediately (either directly or through a H-bond chain) extracts a hydrogen from a neighboring coordinated water, creating another  $\text{OH}^-$  ligand. Since this uses another electron from iron,  $\text{Fe}^{\text{IV}}$  is created. The two  $\text{OH}^-$  ligands rearrange to a water ligand and an oxido ligand, creating the  $\text{FeO}^{2+}$  ion



Iron(IV)oxido species are also found in other types of systems. In heme-containing enzymes like P450,<sup>14</sup> ironoxido species have long been accepted as intermediates, and such intermediates are also regularly found in non-heme iron enzymes.<sup>15–17</sup> The literature covering these enzyme processes is extensive and includes many calculations (see, for example, refs 18–21). Inspired by these biochemical FeO systems, some specific multidentate ligands have been designed to form ironoxido compounds, and indeed ironoxido formation has been found in these systems.<sup>22–24</sup> However, we note that all synthetic ironoxido compounds have a low-spin ground state, unlike the aqueous  $\text{FeO}^{2+}$  studied in the present work ( $S = 1$  vs  $S = 2$ ). Recently though, the high-spin  $[\text{FeO}(\text{H}_2\text{O})_5]^{2+}$  studied here has also been characterized experimentally.<sup>25</sup>

In that paper,<sup>25</sup> Pestovsky et al. claim that  $\text{FeO}^{2+}$  cannot be the active species in Fenton chemistry, because the resulting products differ, but it has been counterargued by Kremer that the experimental evidence is consistent with an  $\text{FeO}^{2+}$  intermediate.<sup>26</sup>

\* Corresponding authors. E-mail: louwerse@few.vu.nl (M.J.L.); baerends@few.vu.nl (E.J.B.).

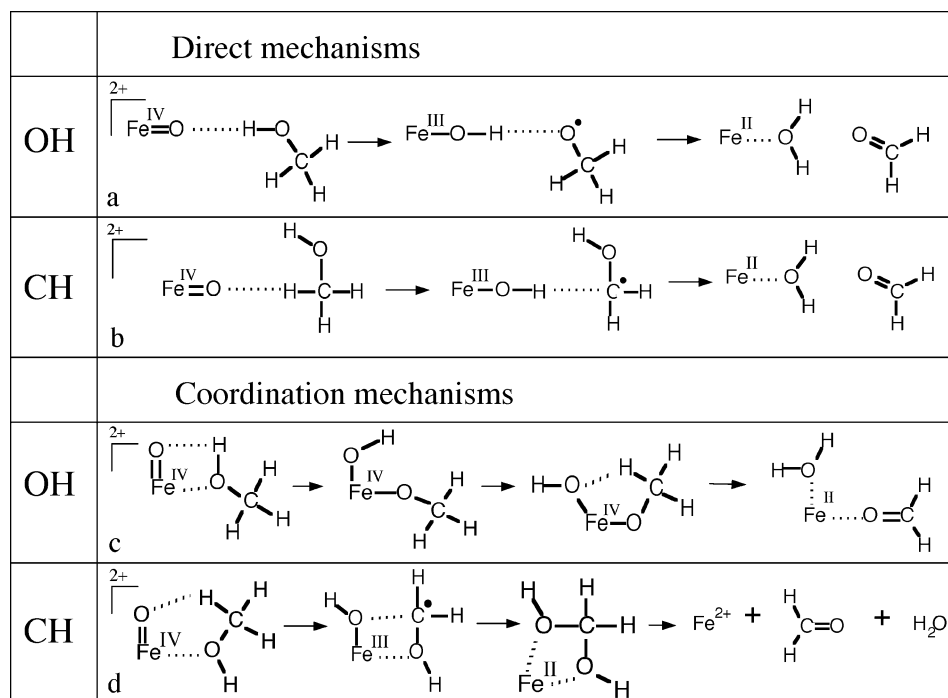
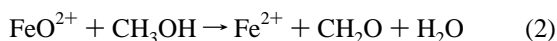


**Figure 1.** Four groups of possible mechanisms for the reaction of  $\text{FeO}^{2+}$  with methanol. For some mechanisms variations are possible because of the influence of the solvent.

Whether or not the ironoxido group is the key intermediate in the Fenton reaction, the reactivity of the  $\text{FeO}^{2+}$  moiety is of considerable interest. In this paper, we study the reactivity of  $\text{FeO}^{2+}$  in water solution, using density functional theory (DFT) and Car-Parrinello simulations. Ensing et al. already studied the reaction with methane,<sup>27</sup> as a prototype for aliphatic hydroxylations, which occur via an H-abstraction/oxygen rebound mechanism as proposed by Groves et al. for aliphatic hydroxylations.<sup>28,29</sup> However, as is also experimentally known, the C–H bond in methane is too strong to make this an efficient reaction. We now investigate the mechanism of another typical reaction for the Fenton reagent: the oxidation of an alcohol to an aldehyde, taking as prototype the oxidation of methanol to formaldehyde. In experimental conditions the reaction continues after the oxidation to formaldehyde eventually producing  $\text{CO}_2$ ,<sup>30</sup> but in our setup, we only concentrate on the first step. In our simulations, there is only one  $\text{H}_2\text{O}_2$  molecule available and the reaction stops at formaldehyde



Most theoretical studies of the oxidation by simple ironoxido systems have focused on the related  $\text{FeO}^+$  species, using the bare (gas phase) species.<sup>31–37</sup> Also the oxidation of methanol to formaldehyde by the bare  $\text{FeO}^+$  has been studied.<sup>33</sup> Recently, the electronic structure of  $\text{FeO}^{2+}$  has been studied for a variety of complexes,<sup>38–45</sup> including  $[\text{FeO}(\text{H}_2\text{O})_5]^{2+}$ .<sup>38</sup> Here, we study oxidation by  $\text{FeO}^{2+}$ , including first-shell water ligands, both in the gas phase and in water solution. The gas-phase calculations are especially useful for precise analyses of the electronic structure aspects of the reaction with  $\text{FeO}^{2+}$  and for comparison with other gas-phase calculations and experiments. The combination of gas-phase calculations and simulations in solution give a remarkable insight into the solvent effects in this reaction.

**Possible Mechanisms.** For the oxidation of methanol to formaldehyde by  $\text{FeO}^{2+}$ , two steps are required: The OH hydrogen atom and one CH hydrogen atom need to be abstracted from the methanol molecule. The possible mechanisms can

roughly be divided into four groups. The first distinction between these groups is that the first step may either be an O–H bond breaking or a C–H bond breaking. The second distinction is whether the first step in the reaction involves direct complexation of methanol to, and reaction with, the oxido oxygen of the  $\text{FeO}^{2+}$  moiety, or whether the first step is a ligand substitution reaction, in which a coordinated water ligand is replaced by methanol. We thus differentiate between a “direct OH mechanism”, a “direct CH mechanism”, a “coordination OH mechanism”, and a “coordination CH mechanism”.

These four possibilities are depicted in Figure 1: In the direct OH mechanism (a) and the direct CH mechanism (b), an H is first transferred to the oxido group, forming a coordinated  $\text{OH}^-$  and an intermediate radical. Next, the other hydrogen is transferred to the coordinated  $\text{OH}^-$  to form an  $\text{H}_2\text{O}$  ligand. In the coordination mechanisms the methanol molecule first coordinates to the iron, replacing a coordinated water molecule. Note that in the coordination OH mechanism (c) the intermediate structure does not involve a radical, because the unpaired electron on the  $\text{CH}_3\text{O}$  fragment combines with an unpaired electron from the Fe ion resulting in a  $\text{CH}_3\text{O}^-$  ligand. Finally, in the coordination CH mechanism (d), the second hydrogen (the OH hydrogen) cannot be transferred directly. In this case, a bond between the just formed OH ligand (bound as  $\text{OH}^-$  to the now formally  $\text{Fe}^{\text{III}}$  ion) and the C atom of the  $\text{CH}_2\text{OH}$  fragment may be formed (cf. the oxygen rebound mechanism in the oxidation of methane to methanol), so that a di-alcohol is formed. This disintegrates in water solution to yield formaldehyde and  $\text{H}_2\text{O}$ .

Also in the direct CH mechanism the di-alcohol could be formed via an oxygen rebound mechanism; however, we find that, in the direct CH mechanism, there is a barrierless second step transfer of the OH hydrogen to the formed OH ligand with which no alternative mechanism could compete.

Some additional variations on the mechanisms could occur when the solvent water molecules are taken into account, because in some cases the hydrogen abstraction can take place via a H-bond chain through the water (as in refs 11–13) or the

solvent water molecules can have other bridging functions. Because of these possible chain mechanisms, it is important to include the solvent water molecules explicitly; simpler models for water like a continuum model or a representation of water–water and water–solute interactions with model potentials, as in MM or QM–MM simulations, can never model such chain reactions correctly.

Finally, there could also be a pH effect on the reaction, because  $[\text{FeO}(\text{H}_2\text{O})_5]^{2+}$  is rather acidic. It is known that the optimal pH range for the Fenton reaction is around pH 3–5,<sup>2,30</sup> and the  $\text{p}K_a$  of  $\text{FeO}^{2+}$  is around  $\text{p}K_a$  2,<sup>46</sup> so deprotonation of a first-shell water molecule may occur during the process. Therefore, we also studied the effect deprotonation of  $[\text{FeO}(\text{H}_2\text{O})_5]^{2+}$  has on the reaction mechanisms.

In this paper, we first study all of these mechanisms in the gas phase, with the first coordination shell of water molecules around the iron ion included in the calculations (microsolvation). Each mechanism that appears viable according to the gas-phase calculations has been studied with large-scale Car-Parrinello simulations at 300 K with 31 water molecules in a periodic box, in addition to  $\text{FeO}^{2+}$  and methanol. We performed thermodynamic integration for each mechanism by doing simulations for a series of fixed (constrained) values of the reaction coordinate, in order to obtain reaction Helmholtz free energies. Finally, the effect on the mechanisms of deprotonation of  $[\text{FeO}(\text{H}_2\text{O})_5]^{2+}$  is studied.

Comparing the gas-phase calculations to the simulations in solution, we find rather large differences. The physical origin of this interesting phenomenon, which is related to differential dielectric screening effects on the one-electron levels of the charged ( $\text{FeO}^{2+}$ ) and neutral ( $\text{CH}_3\text{OH}$ ) reactants, has been further explored, and full details can be found elsewhere.<sup>47</sup>

## 2. Methods

Both the microsolvated gas-phase calculations and the Car-Parrinello simulations were performed with DFT, using the BLYP<sup>48,49</sup> density functional. This functional was chosen because it performs well for liquid water,<sup>50</sup> and it has been shown to be a good choice for calculating reaction energies and transition states for transition metal complexes.<sup>51</sup> Although it has been shown that most functionals of this type tend to underestimate the relative stability of high spin states,<sup>45,52,53</sup> this is not a problem here, because the spin state is constant ( $S = 2$ ) throughout all our calculations.

The (microsolvated) gas-phase calculations were performed with the ADF (Amsterdam density functional) package,<sup>54–57</sup> with all electrons included in the calculations, and using large Slater type orbital (STO) basis sets: a quadruple- $\zeta$  basis set with four sets of polarization functions (QZ4P) for iron and triple- $\zeta$  basis sets with two sets of polarization functions (TZ2P) for the other atoms. The calculations were corrected for relativistic effects using the zero-order regular approximation (ZORA)<sup>58</sup> approach.

In the gas-phase calculations, the first coordination shell of water around the iron ion was included in the calculations (microsolvation). The iron ion is 6-fold coordinated, so 5 water molecules were taken into account in the calculations of the direct mechanisms and 4 water molecules in the coordination mechanisms.

All geometries were fully optimized, and the transition states were determined and characterized in the usual way. Reaction coordinates were also calculated for the transition states, for comparison with the simulations in solution.

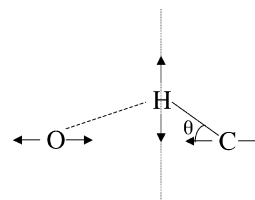


**Figure 2.** Picture of the constraint on reaction coordinate  $\xi$ .

The Car-Parrinello molecular dynamics simulations were performed with the PAW package, using the projector augmented wave method.<sup>59</sup> We used a system consisting of one  $\text{FeO}^{2+}$  ion, one methanol molecule, and 31 water molecules in a periodic cubic box of 10.1 Å, with all hydrogen atoms replaced by deuterium isotopes. The MD time step was 6.5 au (0.157 fs), and the fictitious mass for the wavefunction dynamics was 100 a.u. At each time step, the time derivatives (fictitious velocities) of the wavefunction coefficients were scaled down with 0.005%, and in some simulations, this was increased to 0.01% or 0.02% in order to keep the system on the Born–Oppenheimer surface. The cutoff for the plane wave basis set was 30 Ry (408 eV) for the wavefunctions and 90 Ry (1225 eV) for the charge density.

The PAW projectors for the atoms were constructed with the PAW atomic setups generation program with the 1s electrons of oxygen and carbon, and the 1s, 2s, and 2p electrons of iron selected as frozen cores. We constructed the following projectors: for hydrogen one s-projector with  $E = -0.24001$  a.u. and  $R = 0.557$  a.u.; for oxygen one s- and two p-projectors with  $E_s = -0.87577$  a.u.,  $E_{p,1} = -0.33159$  a.u.,  $E_{p,2} = 0.27777$  a.u., and  $R = 1.267$  a.u.; for carbon one s- and two p-projectors, with  $E_s = -0.50018$  a.u.,  $E_{p,1} = -0.19248$  a.u.,  $E_{p,2} = 0.27777$  a.u., and  $R = 1.33$  a.u.; and for iron two s-, two p-, and three d-projectors with  $E_{s,1} = -3.44446$  a.u.,  $E_{s,2} = -0.19193$  a.u.,  $E_{p,1} = -2.19899$  a.u.,  $E_{p,2} = 2.226$  a.u.,  $E_{d,1} = -0.272$  a.u.,  $E_{d,2} = 0.32717$  a.u.,  $E_{d,3} = 2.0$  au,  $R_{\text{core}} = 1.458$  a.u., and  $R = 1.658$  a.u.

This set of parameters (without using friction on the wavefunction dynamics) was tested for liquid water and produced a stable constant energy (NVE) simulation, conserving the total energy to within 0.005 hartree for a simulation length of 2 ps. The frictions on the wavefunction dynamics were necessary because in the current system the band gaps are often much smaller than in liquid water. The same settings have been used previously in simulations of the OH radical in water.<sup>60,61</sup>

To obtain Helmholtz free energy differences in solution, we performed thermodynamic integrations<sup>62</sup> with the relative position of the abstracted H atom between the methanol and the oxido oxygen as the constrained reaction coordinate,  $\xi$ . For instance, for the CH mechanisms

$$\xi = \frac{R_{\text{CH}} \cos \theta}{R_{\text{CO}}} \quad (3)$$

where  $R_{\text{CH}}$  is the C–H bond distance,  $R_{\text{CO}}$  the C–O bond distance, and  $\theta$  the angle between these bonds (Figure 2). Note that the C–O distance itself is not constrained, and the hydrogen atom can still move freely in the plane perpendicular to the C–O bond. Typically, the value for this constraint changes from 0.3 to 0.7 during the first reaction step. We did constrained simulations at all intermediate values of  $\xi$  with steps of 0.05 and integrated over the constrained force to obtain Helmholtz free energies.

This type of calculation is very sensitive to hysteresis: the force of constraint at a specific value of the reaction coordinate

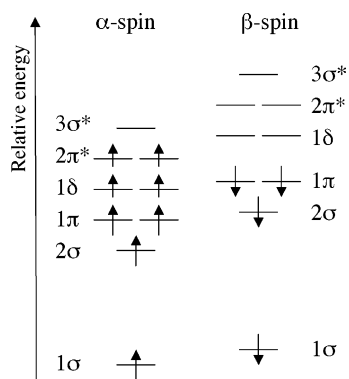


Figure 3. Qualitative molecular orbital scheme for  $\text{FeO}^{2+}$ .

is often different along the forward path (stepwise increase of the reaction coordinate) to that along the reverse path (stepwise decrease of the reaction coordinate);<sup>63</sup> this is caused by the tendency of the solvent to respond very slowly to changes in the reaction coordinate. To minimize the hysteresis, we used relatively long equilibration periods after each change in the reaction coordinate. To be able to estimate the hysteresis properly, we did the simulations strictly in consecutive order: the equilibration at  $\xi = 0.5$  was started from the endpoint of the equilibration at  $\xi = 0.45$ , which was started from the endpoint of the equilibration at  $\xi = 0.4$ , and so on. Furthermore, we simulated one series (the direct OH mechanism) in both forward and backward order to quantify the hysteresis by comparing the two series.

The scheme used for the equilibration was as follows: Each new constraint value was reached by slowly changing the reaction coordinate,  $\xi$ , during 1000 time steps (0.157 ps). The temperature was restored to  $T = 300$  K by employing a thermostat on the ionic degrees of freedom with an oscillation period of 7500 a.u. and a friction on the Nosé variable of 0.05. This thermostat was used for 4 ps, followed for 2 ps by a thermostat with an oscillation period of 60000 a.u. and a friction of 0.001. The latter thermostat was also used for the data collection in simulations ranging from 3 to 14 ps in length.

Strictly speaking, constrained simulations are not sampling a true NVT ensemble but a constrained NVT ensemble, which can slightly bias the constraint force. Therefore, we corrected for this bias with the method of refs 64 and 65 before calculating the statistical averages.

Standard errors were estimated using the method given in ref 66: In molecular dynamics simulations, most fluctuations are caused by thermal movement, so the standard error cannot directly be calculated from the standard deviation. The method used is to take block averages over 1, 2, 4, 8, 16, etc. data points and then the standard deviation of these block averages is calculated. When the resulting standard errors are plotted against the size of the blocks, the curve forms a plateau and the value of this plateau gives the correct statistical standard error.

### 3. Results for Microsolvated $\text{FeO}^{2+}$ in the Gas Phase

First, we will discuss the microsolvated ironoxido species  $[\text{Fe}^{\text{IV}}\text{O}(\text{H}_2\text{O})_5]^{2+}$  and its propensity for complexation with reactants. A full analysis of the orbitals and the orbital energies in  $[\text{Fe}^{\text{IV}}\text{O}(\text{H}_2\text{O})_5]^{2+}$  can be found in ref 38. A schematic picture for  $\text{FeO}^{2+}$  is shown in Figure 3.

The ironoxido species, with its 2+ charge, has a very low-lying LUMO (the  $\alpha$ -spin  $3\sigma^*$  orbital), which makes it a very strong electron acceptor. Although the empty  $\beta$ -spin 3d ( $1\delta$ ) orbitals are even lower in energy, they are not as important

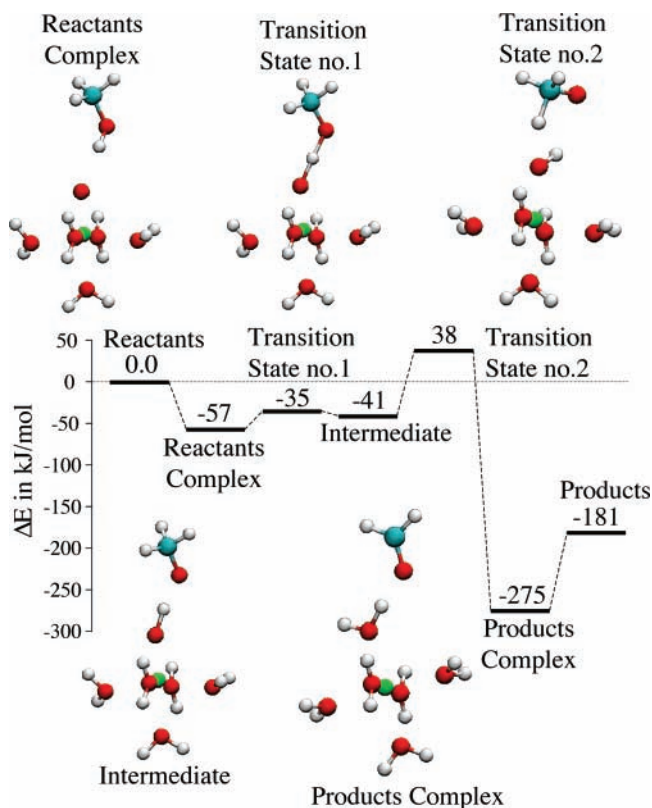
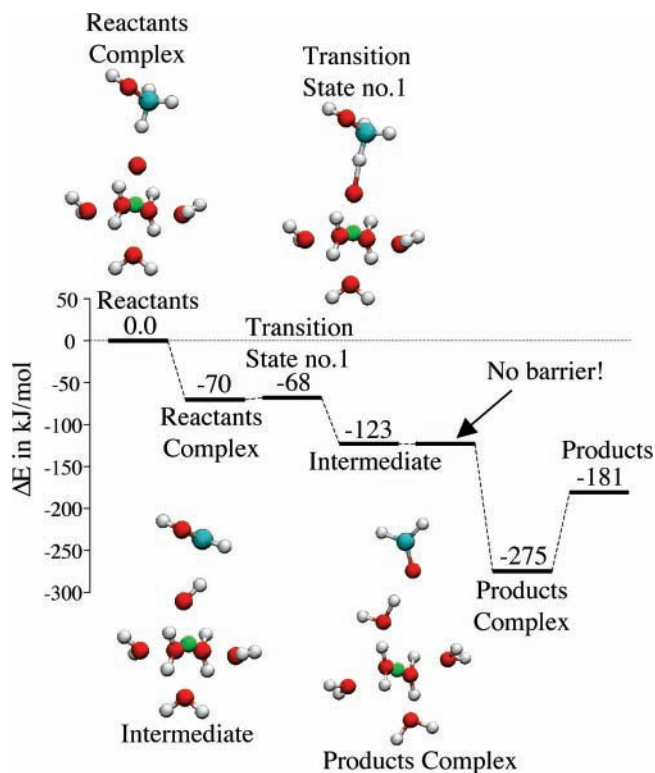


Figure 4. Microsolvated gas-phase results for the direct OH mechanism.

because they are shielded by the water ligands and, thus, not accessible for interactions. The  $\alpha$ -spin  $3\sigma^*$  orbital, the  $\sigma^*$  antibonding combination of the Fe-3d<sub>z<sup>2</sup></sub> orbital and the O-2p<sub>z</sub> orbital (with the Fe–O bond chosen as the  $z$  axis), reaches spatially beyond all the occupied orbitals on the oxygen side;<sup>47</sup> therefore, it is of particular interest when any molecule approaches the ironoxido oxygen. Normally, one would expect the oxygen atom to act as a hydrogen bond acceptor, but when a potential hydrogen bond donor approaches, its O–H  $\sigma$  bond orbital will start to overlap with the strongly electron-withdrawing  $\text{FeO}^{2+}$  LUMO. As a result, a  $\sigma(\text{OH}) \rightarrow 3\sigma^*(\text{FeO}^{2+})$  charge transfer interaction will occur rather than the formation of a hydrogen bond, which is characterized by the reverse charge transfer ( $\text{O}-\text{lp} \rightarrow \sigma$ ).

As a result, complexation to the oxido oxygen does not show any preference for H-bond donating groups, and, moreover, the interactions are much stronger than for hydrogen bonds. Strong charge transfer interactions with the  $3\sigma^*$  orbital occur even more readily for C–H bonds or oxygen lone pairs than for the lower lying O–H bond orbitals: For water we find an interaction energy via an oxygen lone pair (so not in H-bonding orientation) of 43 kJ/mol, and methanol binds via its OH group with 57 kJ/mol (see Figure 4) and via a C–H bond even with 70 kJ/mol (see Figure 5). These interaction energies already suggest that  $[\text{FeO}(\text{H}_2\text{O})_5]^{2+}$  will indeed abstract hydrogen atoms very easily, and can be expected to have a preference for C–H bonds over O–H bonds. We refer to ref 47 for a detailed investigation of these electronic structure features of the interaction of  $[\text{FeO}(\text{H}_2\text{O})_5]^{2+}$  with organic substrate molecules.

(a) **Direct Mechanisms in the Gas Phase.** The results for the direct OH mechanism in the microsolvated gas phase are given in Figure 4 and for the direct CH mechanism in Figure 5. The first step of the direct OH mechanism, the abstraction of the OH hydrogen, has a relatively small barrier of 22 kJ/mol



**Figure 5.** Microsolvated gas-phase results for the direct CH mechanism. The second step has no barrier, so the intermediate structure is not a fully optimized minimum but a configuration where the energy surface is almost flat. Energies are given in kJ/mol.

relative to the reactants complex, with the transition state at reaction coordinate  $\xi = 0.51$ . However, the intermediate product, a  $\text{CH}_3\text{O}$  radical complexed to  $[\text{FeOH}(\text{H}_2\text{O})_5]^{2+}$ , is only stable by 6 kJ/mol with respect to the transition state and is still unstable by 16 kJ/mol with respect to the reactants complex. Furthermore, the barrier of the second step, the abstraction of the methyl H, is rather high (79 kJ/mol), rendering the direct OH mechanism in the gas-phase unlikely, though not impossible.

The direct CH mechanism, on the other hand, hardly shows any barrier in the microsolvated gas-phase calculations. The first step, the abstraction of a methyl hydrogen atom, has a barrier of less than 2 kJ/mol (at reaction coordinate  $\xi = 0.45$ ). In the transition state the incipient formation of the flat  $\text{CH}_2\text{OH}$  radical is visible (see transition state no. 1 in Figure 5). After crossing this low barrier, the energy goes down by some 54 kJ/mol and the flat  $\text{CH}_2\text{OH}$  radical is formed; however, a stable intermediate structure is not reached because the second step, the abstraction of the hydroxyl hydrogen, appears to have no barrier at all: When the intermediate structure with the  $\text{CH}_2\text{OH}$  radical is optimized, the hydroxyl H rotates toward the FeOH, and it is abstracted spontaneously, even in a regular geometry optimization calculation. The energy and geometry of the intermediate structure presented here are thus only estimates based on the region of phase space where the energy surface is almost flat.

It should be noted that this second step is different from the so-called oxygen rebound type mechanism, which is familiar from heme iron oxidation catalysis and also operates in methane oxidation by the  $\text{FeO}^{2+}$  ion.<sup>27</sup> That mechanism also starts with the abstraction of an aliphatic H. However, the newly formed OH group then binds to the carbon atom of the organic radical, retaining a (weaker) coordination bond to the Fe by way of the oxygen lone pair of the formed alcohol. In the current case, in which an OH group is already present, this would mean that a di-alcohol would be formed (which would yield formaldehyde

by splitting off a water molecule). However, from our findings, it appears that for the oxidation of a primary alcohol, after the formation of the  $\text{CH}_2\text{OH}$  fragment, it is easier to transfer the hydroxyl H to FeOH to form a water ligand and the RCHO product.

In the products complex, the formaldehyde molecule binds rather strongly (93 kJ/mol) to the newly formed water ligand, much stronger than by a simple hydrogen bond. This phenomenon has been observed before<sup>10</sup> for complexation by “hydrogen bonding” of a second sphere molecule to a first sphere water ligand of the strongly positive charged  $\text{Fe}(\text{H}_2\text{O})_6^{2+}$  complex. The bond is much stronger than a normal hydrogen bond because both the electrostatic contribution and the donation into the O–H  $\sigma^*$  orbital of the coordinated  $\text{H}_2\text{O}$  become much larger.

In conclusion, based on our microsolvated gas-phase calculations, the direct CH mechanism seems to have high probability, with a spectacularly low barrier. This very low barrier (strikingly lower than for H abstraction from the hydroxyl group) is caused by the strong charge transfer from the C–H bond orbital into the  $\text{FeO}^{2+}$  LUMO. This charge transfer already exists in the reactants complex and increases strongly as the C–H bond lengthens, since the  $\sigma(\text{C–H})$  orbital rises in energy. The charge transfer interaction of  $\sigma(\text{C–H})$  with the  $\text{FeO}^{2+}$  LUMO is then enhanced, which compensates for much of the strain energy of stretching the C–H bond. This is a typical orbital mechanism for bond breaking/forming.

**(b) Coordination Mechanisms in the Gas Phase.** For the complexation of methanol to the oxido oxygen in the direct mechanisms, we found unexpectedly strong charge transfer interactions, in particular for approach with a C–H bond. For coordination to the iron, however, it is no surprise to find strong coordinative bonds. In fact, the coordination to Fe is much stronger than the complexation to the oxido oxygen: When the methanol molecule coordinates with its OH group next to the oxido oxygen, which is the right configuration for the coordination OH mechanism (Figure 1c), the coordinative bond energy is 150 kJ/mol. When the methanol coordinates with the  $\text{CH}_3$  group next to the oxido oxygen, the configuration for the coordination CH mechanism (Figure 1d), it is 154 kJ/mol. However, to make coordination to the iron ion possible, a strongly bound water molecule first needs to be removed, which costs 110 kJ/mol in the gas phase (N.B. these three gas-phase values were calculated with 4 additional water ligands coordinated to the iron).

The results for the coordination OH mechanism in the microsolvated gas phase are given in Figure 6. The first step (after coordination) is again the abstraction of the hydroxyl hydrogen, but in the case of coordinated methanol, this abstraction has a high barrier of 103 kJ/mol. In the coordination CH mechanism, the first step also has a high barrier, namely 95 kJ/mol. Apparently, in both cases, coordinated methanol cannot make the right angle with the Fe–O bond and does not have sufficient overlap with the LUMO, which is a  $\sigma$  orbital along the FeO axis, to become activated for hydrogen abstraction. As a result, these barriers are too high to give reasonable mechanisms.

However, in the case of the coordination OH mechanism, a bridging water molecule, which is hydrogen bonded to the methanol hydroxyl group, could lower the barrier via a concerted reaction (Figure 7): When the coordinated methanol molecule makes a hydrogen bond to a water molecule from the solution, this water molecule could in turn interact with the LUMO, with its high amplitude at the oxido site. Then, while the ironoxido abstracts an H from the water, the water could in turn abstract

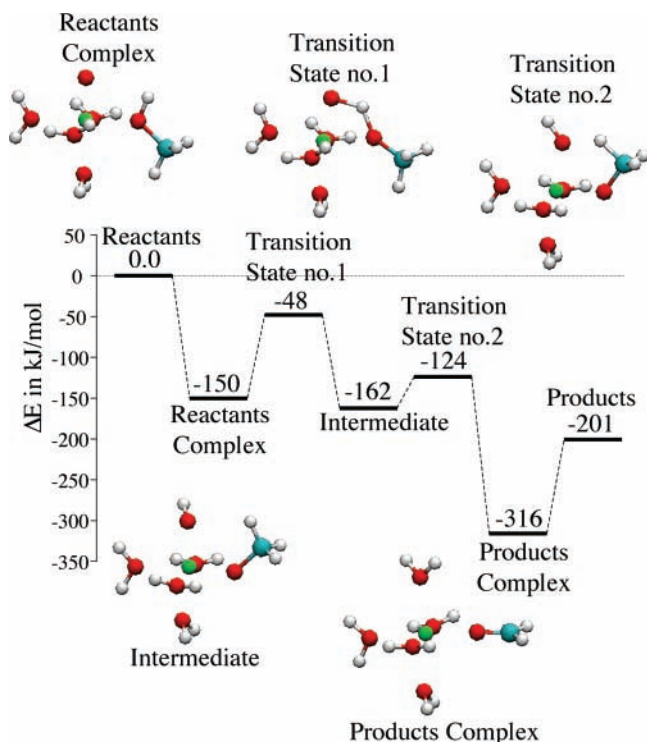


**Figure 6.** Microsolvated gas-phase results for the coordination OH mechanism. Note that the zero-level (the free reactants) includes a vacant coordination site.

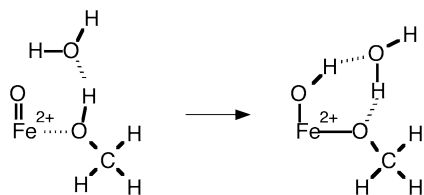


**Figure 7.** First step of the coordination OH mechanism that can be facilitated by an additional bridging water molecule. The barrier is lowered considerably by the bridging function of the water molecule from 103 to 31 kJ/mol. In this case it is not a hydrogen atom but a proton that is transferred.

the hydrogen of the methanol OH group. This would be facilitated by the coordination of the methanol OH group to the iron, since a strong coordinative bond to the resulting  $\text{CH}_3\text{O}$  radical could be formed (forming a (formally)  $\text{CH}_3\text{O}^-$  ligand). We find, however, that the reaction occurs in two discernible steps and starts at the coordinated methanol: first an H is transferred to the intermediary water, and then the transfer of (another) H from the water to the oxido takes place. The two barriers have practically the same height, with a very shallow minimum in between. The height of the barriers is only 31 kJ/mol, much reduced compared to the 103 kJ/mol of the direct transfer of the hydroxyl H to the oxido.

The end result of this step is formally an  $\text{Fe}^{\text{IV}}$  ion with an  $\text{OH}^-$  ligand and a  $\text{CH}_3\text{O}^-$  ligand. This situation can be reached simply by heterolytic splitting of the O–H bond of methanol, the resulting  $\text{H}^+$  being transferred to the formally 2-oxido group to form  $\text{OH}^-$ , leaving  $\text{CH}_3\text{O}^-$  behind. Alternatively, a homolytic splitting would result in  $\text{CH}_3\text{O}^\bullet$  and a hydrogen atom. The latter would supply an additional electron to the oxido group. In order for the  $\text{OH}^-$  ligand to be formed, the electron would have to move to the Fe center and then to  $\text{CH}_3\text{O}^\bullet$  to generate the  $\text{CH}_3\text{O}^-$  ligand. On the Born–Oppenheimer surface, such electron redistributions do not occur in time but simultaneously with the changes of the atomic positions. Since the electron density

is easily redistributed in the complex during the reaction, it is not easy to establish which one of these two pictures is more accurate. We find that the transferred hydrogen (from methanol to the water molecule) bears no spin polarization (0.03) but also does not have a full positive charge: The charge increase of the  $\text{H}_3\text{O}^{\delta+}$  compared to the charge of the water molecule before the reaction (+0.2) is only +0.5 according to Mulliken<sup>67</sup> and +0.3 according to Hirshfeld<sup>68</sup> and Voronoi<sup>69</sup> charge analyses. When the (other) H of  $\text{H}_3\text{O}^{\delta+}$  moves on to the oxido oxygen, the charge on the  $\text{H}_2\text{O}$  molecule drops to +0.2 again. It appears that the picture of  $\text{H}^+$  dissociation from methanol is not wrong. It should be kept in mind that the redistribution of charge (due to small changes in the many orbitals that build the total charge density) prevents the development of full (almost integer) charges. In fact, precisely the same happens if we put a proton in a water solution. We have found in Car-Parrinello simulations of a proton in water that the proton continuously forms a  $\text{H}_3\text{O}^{\delta+}$  ion, with  $\delta^+ = +0.43 \pm 0.02$ . The present charge analyses therefore suggest that heterolytic splitting of the O–H bond takes place.

The second step in the coordination OH mechanism is the transfer of a methyl H to the just formed  $\text{OH}^-$  ligand. Since a neutral  $\text{H}_2\text{O}$  ligand is formed and a neutral formaldehyde ligand, formally two electrons go to Fe, changing  $\text{Fe}^{\text{IV}}$  into  $\text{Fe}^{\text{II}}$ . The barrier for this methyl H transfer is not very high (38 kJ/mol at reaction coordinate  $\xi = 0.46$ ).

In conclusion, the microsolvated gas-phase calculations suggest that, with a bridging water molecule facilitating the first step, the coordination OH mechanism is possible. This mechanism is thus also considered in the Car-Parrinello simulations.

For the coordination CH mechanism, it is not possible to lower the H abstraction barrier with a bridging water molecule, because the C–H bond does not form hydrogen bonds with the water molecules. The coordination CH mechanism is therefore not considered any further.

For easy reference, we collect all of the results for the microsolvated system in the gas phase in Table 1, as well as the Car-Parrinello results and the results for the deprotonated system to be discussed in a later section.

#### 4. Car-Parrinello Results

For the fully solvated systems in solution, first the stability of the reactant complexes for the direct mechanisms was studied. We equilibrated the solvent and the reactant complexes while constraining the distance between the methanol molecule and the ironoxido molecule and followed this by unconstrained simulations to investigate whether the complexes are stable in solution. We did two simulation runs: one starting with the hydroxyl oxygen constrained at 2.92 Å from the oxido oxygen and another starting with the carbon atom constrained at 2.96 Å from the oxido oxygen. Interestingly, we found that, when the constraints are removed, the methanol molecule diffuses slowly away from the  $\text{FeO}^{2+}$  molecule, into the solution. This happens both when the methanol is interacting with  $\text{FeO}^{2+}$  via its OH group and when it interacts via its  $\text{CH}_3$  group.

Apparently, the  $\text{FeO}^{2+}$ –methanol complex is not stable in solution, in spite of the very strong interaction in the gas phase. Of course, the  $\text{FeO}^{2+}$ –methanol bond now has to compete with an  $\text{FeO}^{2+}$ –water bond (minus the difference between hydrated methanol and hydrated water) and the entropy will favor the methanol going into the solution. Still, in view of the strong bond (70 kJ/mol) of the methyl group to ironoxido in the gas phase, one would expect this bond to prevail (the  $\text{FeO}^{2+}$ –water bond is “only” 43 kJ/mol in the microsolvated gas phase). It



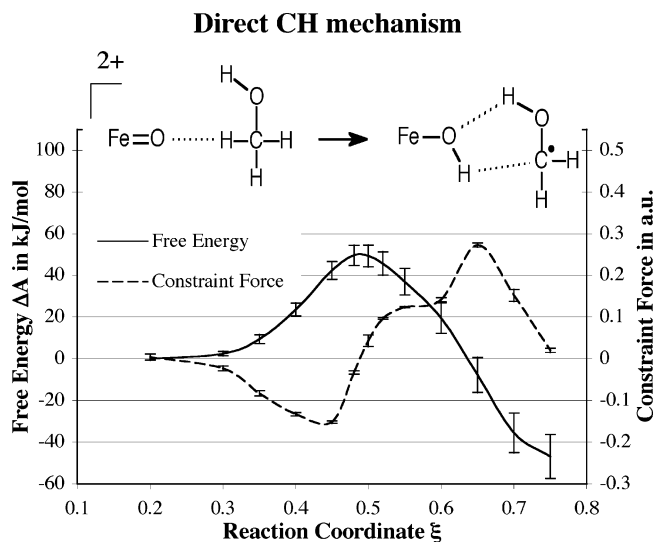


**Figure 9.** Thermodynamic integration results for the direct CH mechanism. At  $\xi = 0.65$  the second step of the reaction spontaneously occurs and there is a large change in the constraint force. The error bars in the free energy curve are based on the hysteresis in the direct OH mechanism and are only indicative.

**(b) Direct CH Mechanism in Solution.** For the direct CH mechanism, we have performed a thermodynamic integration along the reaction coordinate describing methyl H transfer to the oxido group; see eq 3. The Helmholtz free energy profile, exhibiting a barrier of  $50 \pm 10$  kJ/mol, and the force of constraint are shown in Figure 9. In the gas phase, it was determined that a structure corresponding to the resulting intermediate radical  $\cdot\text{CH}_2\text{OH}$  complexed to the  $\text{FeOH}^{2+}$  group could not be optimized, since transfer of the hydroxyl H to form  $\text{Fe}(\text{H}_2\text{O})^{2+}$  occurred spontaneously. We found something similar in the MD simulations of the process in solution. At  $\xi = 0.65$ , which is well beyond the transition state for C–H bond breaking, see Figure 9 (i.e., the transfer of the CH hydrogen to the  $\text{FeO}^{2+}$  is almost complete), the OH hydrogen leaves into the solution. It travels through the solvent via a chain mechanism (Figure 10) to end up on the former oxido oxygen (now the O of the OH ligand), resulting in  $[\text{Fe}(\text{H}_2\text{O})_6]^{2+}$  and formaldehyde. As a result of the occurrence of this “second step”, the constraint force required to keep the CH hydrogen in the position dictated by the reaction coordinate value ( $\xi = 0.65$ ) suddenly increases, because beyond this point a completely different situation is modeled.

The OH hydrogen (the “second step”) diffuses through the solvent by a Grotthuss diffusion mechanism (Figure 10) until it ends up at the oxido in a neighboring cell (as periodic image of the H that ends up at the oxido of the central unit cell, see last snapshot of Figure 10). In the periodic system used in these simulations, the diffusion path runs to the OH ligand in the neighboring cell, but it could also have formed a loop to the OH ligand at its own Fe ion. In dilute solutions, that would certainly be the case. This is actually very similar to the situation we have found in the O–O bond breaking of a coordinated  $\text{H}_2\text{O}_2$  molecule, where an OH ligand is formed and the OH radical that is produced reacts through a H-bond wire either with a water ligand at the neighboring Fe or at the same Fe.<sup>11,12</sup> The statistics for these processes are an issue in these Car-Parrinello simulations with relatively small unit cells, a point that has been extensively investigated using the transition path sampling technique.<sup>13</sup>

It is interesting to consider in what nature the hydrogens are transferred: as proton, hydrogen atom, or hydride ion. The

atomic charges and spin densities have been analyzed in the two different ways offered in the software package. The atomic charges are followed during the simulations using a built-in function of the PAW package that fits the charge density with Gaussian functions located at the atomic centers. A reasonable description of the atomic charges is obtained with 2 Gaussians per atom and a fitting cutoff of 5 Ry. The resulting charges should not be interpreted quantitatively, but they do provide a good opportunity to monitor changes in the electronic charge distribution in the system. Because the atomic charges are available for each MD step, the fluctuations in the charges can be analyzed as well.

For the atomic spin densities, the (delocalized) orbitals are expanded in spherical harmonics and separated into up- and down-spin. The difference yields the local spin densities, recovering around 90% of the total spin.

The charge and spin density analyses do not lead to clear-cut, (almost) integer values for electron and spin densities on the transferring hydrogens, as was observed previously for the coordination OH mechanism in the gas phase. When the methanol binds to the ironoxido ( $\xi = 0.3$ ) it obtains a small charge of  $+0.139 \pm 0.008$  and a very small net spin of  $+0.005$ . During the transfer of the CH hydrogen a more significant (negative) spin and a positive charge start to accumulate on the  $\cdot\text{CH}_2\text{OH}$  moiety that is left behind. At  $\xi = 0.65$  the  $\text{CH}_2\text{OH}$  has a charge of  $+0.347 \pm 0.015$  and a net spin of  $-0.32$ . So there is a tendency to form a  $\cdot\text{CH}_2\text{O}$  radical, but there is, apparently, still considerable interaction with (charge transfer to) the  $\text{FeOH}^{2+}$  group, leading to a net charge of  $+0.35$ . The build up of a full  $-1$  spin is counteracted by reorganization of the “spectator” orbitals (not directly involved in the bond breaking process) and by the extent to which the charge transfer (from the  $\cdot\text{CH}_2\text{O}$  radical) consists more of  $\beta$  spin density than  $\alpha$  spin density. When next the OH hydrogen leaves into the solution, the charge and the spin on the formed  $\text{CH}_2\text{O}$  drop again to  $+0.09 \pm 0.02$  (charge) and  $-0.13$  (spin), leaving a practically closed shell  $\text{CH}_2\text{O}$  moiety complexed to the FeOH (still at  $\xi = 0.65$ ). Finally, the  $\text{H}_3\text{O}$  molecules that are formed during the H transfer through the solvent (Figure 10) have a net spin of 0.000 and a charge of  $+0.36 \pm 0.08$  (for comparison: not reacting water molecules in this simulation have a charge of  $+0.03 \pm 0.05$ ).

Although these results are not unequivocal, they justify in our view the interpretation that in the “first step”; indeed, an  $\text{H}^\cdot$  radical is transferred and a  $\cdot\text{CH}_2\text{OH}$  radical is formed. The interaction of the  $\cdot\text{CH}_2\text{OH}$  with FeOH apparently still involves considerable charge transfer. With respect to the nature of the second H, it is hard to decide unambiguously whether the picture that it transfers as  $\text{H}^\cdot$  (just like the first H) or as  $\text{H}^+$  is most appropriate. It should be kept in mind that in the solvent there will always be considerable charge flow into the 1s orbital of the  $\text{H}^+$ , as well as other charge rearrangements, compensating much of the formal  $+1$  charge. As mentioned before, CPMD simulations of a proton in water solution yield a charge of  $+0.43 \pm 0.02$  el. This suggests that we are most probably dealing with an  $\text{H}^+$ . Of course, when  $\text{H}^+$  leaves, an (almost) neutral  $\text{CH}_2\text{O}$  is left behind, so an additional electron must be transferred from  $\text{CH}_2\text{O}$  to the Fe complex. The calculated charge and spin densities show that the charge rearrangements are rather subtle and we should beware of oversimplistic interpretations.

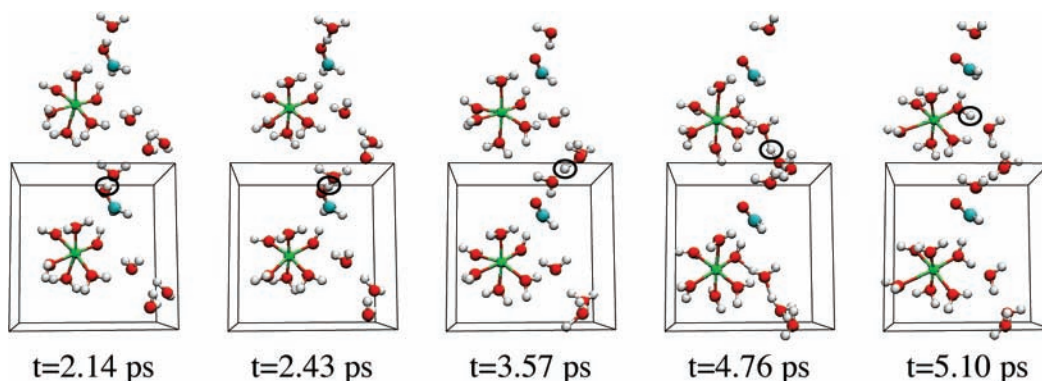


**Figure 10.** Snapshots from the simulation at  $\xi = 0.65$  in the direct CH mechanism. As visible in the snapshots a reaction coordinate  $\xi = 0.65$  corresponds to almost complete transfer of the H to the oxido oxygen. In this simulation the OH hydrogen of methanol moves into the solution and travels via a chain mechanism to the iron complex. This second step occurs spontaneously already, while the first step of the reaction has not finished yet. In the pictures the unit cell is shown plus one periodic image. The water molecules that are not taking part in the proton transfer and that are not coordinated to the iron are left out of the pictures. The hydrogen of interest has been circled.

In our simulations the “second step” of H dissociation from  $\text{CH}_2\text{OH}$  occurs spontaneously. This is reminiscent of situations where, owing to an improper choice of reaction coordinate, one first climbs too strongly uphill out of the reactants basin along the chosen reaction coordinate only to “escape” suddenly to the products basin along an orthogonal coordinate. Typically, a lower transition state could then be found if the intrinsic reaction coordinate were to be followed. It is not so clear whether this circumstance applies here. In theory, rather than pushing the system along the chosen reaction coordinate (i.e., transferring the methyl H to oxido) until the spontaneous transfer of the hydroxyl H occurs, a different reaction coordinate, which would start to deviate from the chosen reaction coordinate at a smaller value of the present  $\xi$  and entail transfer of the two Hs in a concerted (or “nonsynchronous concerted”<sup>70</sup>) process, could lead to an overall lower reaction barrier. In particular this would be the case if the intrinsic reaction coordinate should deviate from the chosen one before the present transition state value of  $\xi = 0.49$ . However, we observe that the H dissociation now occurs well beyond the transition value of  $\xi = 0.49$ ;  $\xi = 0.65$  is well beyond the transition state at a free energy that is lower than that of the reactants. Therefore, even though we cannot rule out the possibility that a better choice of reaction coordinate would yield a lower barrier, we do not consider this very likely. We are aware, though, that our barrier free energy of 50 kJ/mol should strictly be considered an upper bound.

The important conclusion remains that the direct CH mechanism is a very likely mechanism for the oxidation by  $\text{FeO}^{2+}$ .

The barrier that we have found is considerably higher than the 2 kJ/mol found in the microsolvated gas phase. This is an interesting solvent effect, which, as mentioned earlier, has an electronic origin: the dielectric screening effects of the solvent lead to a relative upshift of the one-electron levels of the 2+ charged Fe complex, most notably the LUMO, which is the major acceptor orbital for charge donation out of the C–H  $\sigma$  bonding orbital of the methyl group. In this way, the solvent weakens the charge transfer interaction between the C–H bond orbital and the  $\text{FeO}^{2+}$  LUMO, which is the main cause of the C–H bond weakening and breaking. This solvent effect has been fully investigated elsewhere.<sup>47</sup>

**(c) Coordination OH Mechanism in Solution.** Finally, we consider the coordination OH mechanism in solution. Earlier, we tested the stability of the reactant complexes in solution for the direct mechanisms. However, coordination to the iron ion is much stronger than complexation to the oxido of  $\text{FeO}^{2+}$ . The (microsolvated) gas-phase calculations show that water mol-

ecules are bound even stronger to the  $\text{Fe}^{\text{IV}}$  of  $\text{FeO}^{2+}$  than for instance to  $\text{Fe}^{2+}$  (117 kJ/mol to  $\text{Fe}^{\text{IV}}$  vs 97 kJ/mol to  $\text{Fe}^{\text{II}}$ ). It is therefore to be expected that there will be barriers to replace a coordinated water molecule by a methanol molecule and vice versa. Indeed, we find that the coordination of a methanol molecule to  $\text{FeO}^{2+}$  in solution is stable for the duration of our simulations (in total ca. 70 ps).

More interesting, however, is the behavior of the OH hydrogen of the coordinated methanol molecule. The methanol becomes rather acidic, even more so than the coordinated water molecules. On the time scale of this type of simulation the probability of spontaneous deprotonation is very small, though. As an indirect indication of the acidity of coordinated methanol we can consider the observed lengthening of the O–H bond: For a free methanol molecule in solution the length of the O–H bond during an MD run is  $0.99 \pm 0.03$  Å, and for coordinated methanol it is  $1.03 \pm 0.05$  Å. For the already quite acidic coordinated water molecule (the  $\text{pK}_a$  of  $\text{FeO}(\text{H}_2\text{O})_5^{2+}(\text{aq})$  has been estimated to be 2), the values for solvated and coordinated water molecules are  $0.99 \pm 0.03$  and  $1.01 \pm 0.03$  Å, respectively. The stronger O–H bond lengthening of the coordinated methanol indicates that it is more acidic. Accordingly, the H atom abstraction of the first reaction step (Figure 1c) can be circumvented in solution by proton transfer through the solvent. As a matter of fact, we have found in the gas-phase that with one intermediate water molecule the H that was transferred along this short chain could not be identified as pure  $\text{H}^\bullet$  or  $\text{H}^+$  in a straightforward manner. In any case, the end result is formally a  $[\text{Fe}^{\text{IV}}\text{OH}]^{3+}$  with a coordinated  $\text{CH}_3\text{O}^-$ , i.e.,  $[\text{Fe}^{\text{IV}}(\text{CH}_3\text{O}^-)(\text{OH}^-)]^{2+}$ . We assume that this H transfer is so facile that it is not a rate-limiting step. The probability of the alternative, the proton staying in the water solution, depends on the concentration of the system; in our small simulation cell this situation has a very low probability as it would lead to an  $\text{H}^+$  concentration of 2M, giving a pH of  $-0.3$ !

So for the thermodynamic integration of the second step of the reaction, the transfer of a methyl hydrogen, we have assumed that H transfer from the hydroxyl group to the oxido oxygen takes place.

The results of the thermodynamic integration of the second reaction step are shown in Figure 11. We find a Helmholtz free energy barrier of  $44 \pm 10$  kJ/mol. The height and the position of this barrier in solution are very similar to the energy barrier of 38 kJ/mol in the gas phase. It is interesting that here we have an example in which solvent effects do not change the barrier significantly.

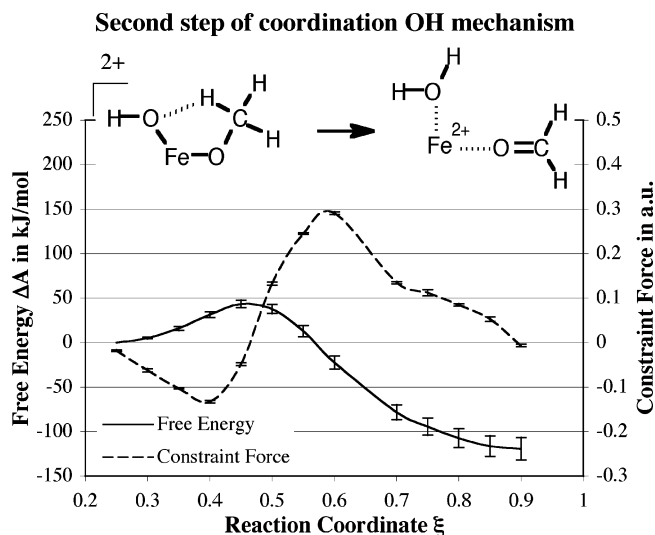


**Figure 11.** Thermodynamic integration results for the second step of the coordination OH mechanism. The error bars in the free energy curve are based on the hysteresis in the direct OH mechanism and are only indicative.

With a barrier of 44 kJ/mol, which is comparable to the 50 kJ/mol of the direct CH mechanism, the coordination OH mechanism seems to have a reasonable probability of occurring. However, the methanol molecule first needs to substitute a water ligand and coordinate to the iron ion, and then its H needs to be transferred via the solvent toward the oxido oxygen, before the second step can take place. Since the competitive direct CH mechanism does not depend on a prior ligand substitution, the barrier for ligand substitution may be an important factor in the preference of one reaction path over the other. Although the coordination OH mechanism cannot be ruled out, since ligand substitution can be fast in spite of strong metal–ligand bonds, we expect that the direct CH mechanism will be the most important one for the oxidation by  $\text{FeO}^{2+}$ .

### 5. Reactions with Deprotonated $[\text{FeO}(\text{H}_2\text{O})_5]^{2+}$

As mentioned before,  $[\text{FeO}(\text{H}_2\text{O})_5]^{2+}$  is rather acidic; the  $\text{pK}_a$  is experimentally unknown but has been estimated at ca. 2.<sup>46</sup> This means that under the usual conditions of the Fenton reaction (optimal pH: 3–5<sup>2,30</sup>) it might be deprotonated. Therefore, we should not only study  $[\text{FeO}(\text{H}_2\text{O})_5]^{2+}$ , but also its conjugate base:  $[\text{FeO}(\text{H}_2\text{O})_4\text{OH}]^+$ . We have thus performed further calculations in the gas phase and in solution. We discuss the direct OH, the direct CH, and the coordination OH mechanism in the gas phase, and the direct OH mechanism in solution.

The complexes have several nonequivalent protons, but because deprotonation has a clear deactivating effect as result of the change in net charge, as shown below, we restricted ourselves to demonstrating the effect for removal of a proton from an equatorial water molecule. For the deprotonated version of the second step of the coordination OH mechanism, we removed the proton from the  $\text{OH}^-$  ligand, which it had formed with the oxido oxygen in the first step. This is equivalent to the assumption that the coordinated methanol is more acidic than the coordinated water molecules, and the deprotonated species to be considered is therefore the one in which the hydroxyl H of methanol has been removed (as  $\text{H}^+$ ), leaving only the second step of this mechanism (transfer of a methyl H to the oxido group) to be investigated.

In the simulations in solution, the same (equatorial) proton was removed as in the gas phase. During these simulations no proton exchange between first-shell water molecules was observed.

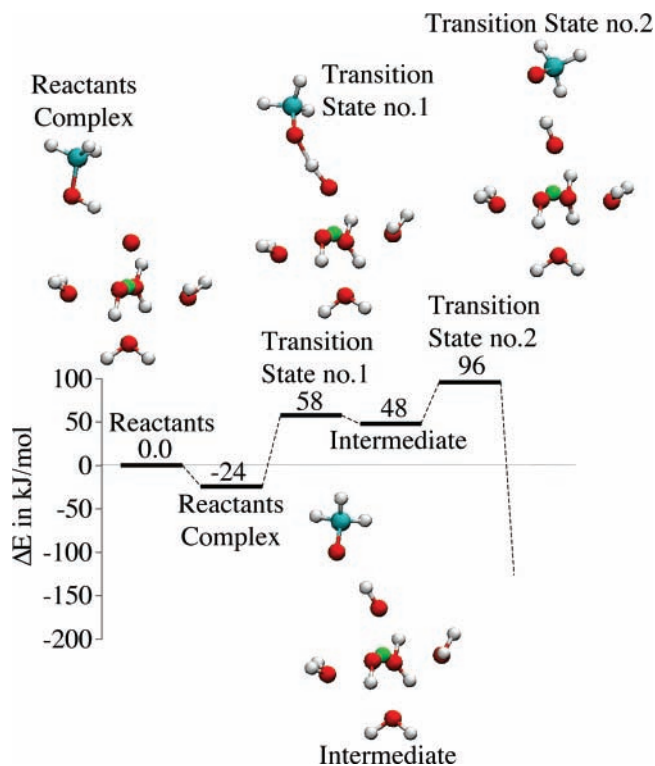


**Figure 12.** Microsolvated gas-phase results for the direct OH mechanism in the deprotonated state. One of the protons of an equatorial water molecule has been removed.

**TABLE 2: Interaction Energies in kJ/mol of  $[\text{FeO}(\text{H}_2\text{O})_5]^{2+}$  with Water and Methanol Compared to the Interaction Energies of Its Conjugate Base Complexes**

	$\text{FeO}-\text{H}_2\text{O}$	$\text{FeO}-\text{HOCH}_3$	$\text{FeO}-\text{H}_3\text{COH}$
$[\text{Fe}^{\text{IV}}\text{O}(\text{H}_2\text{O})_5]^{2+}$	43 (OO-bond)	57	70
$[\text{Fe}^{\text{IV}}\text{O}(\text{H}_2\text{O})_4\text{OH}]^+$	21 (H-bond)	24	5

(a) **Gas Phase.** Going from  $[\text{FeO}(\text{H}_2\text{O})_5]^{2+}$  to  $[\text{FeO}(\text{H}_2\text{O})_4\text{OH}]^+$ , the orbitals shift upward in energy, and the LUMO is not that extremely low in energy anymore. As a result, the charge transfer interaction with a substrate (methanol or water) is strongly diminished. In fact, the reactants can now form hydrogen bonds, with the oxido oxygen acting as electron donor ( $\text{H}$ -bond acceptor) by way of the half filled  $2\pi^*$  orbitals. The interaction energies drop to 21 kJ/mol for water (now hydrogen bonded), 24 kJ/mol for methanol via the OH group (much closer to typical H-bond strengths), and a mere 5 kJ/mol when methanol interacts via its  $\text{CH}_3$  group, which of course is a very poor H-bond donor (Table 2).

In Figure 12, the gas-phase results are given for the direct OH mechanism with deprotonated  $\text{FeO}^{2+}$ . As shown in Table 2, the complexation at  $[\text{FeO}(\text{H}_2\text{O})_4\text{OH}]^+$  is much weaker, caused by the fact that the charge transfer interaction is replaced by a classical hydrogen bond interaction. As a result, the barrier for the abstraction of the OH hydrogen also increases. This barrier becomes rather high (82 kJ/mol at reaction coordinate  $\xi = 0.55$ , compared to 22 kJ/mol before), and the second barrier is also considerable, making the reaction less favorable when the ironoxido complex is in a deprotonated state.

For the direct CH mechanism, the most probable mechanism when  $\text{FeO}^{2+}$  is not deprotonated, the change is even more dramatic (not depicted): In this case, the energy of complexation is reduced from 70 to 5 kJ/mol, and the barrier of the methyl H-abstraction increases from 2 to 39 kJ/mol. The second barrier, the abstraction of the hydroxyl hydrogen, even changes from 0

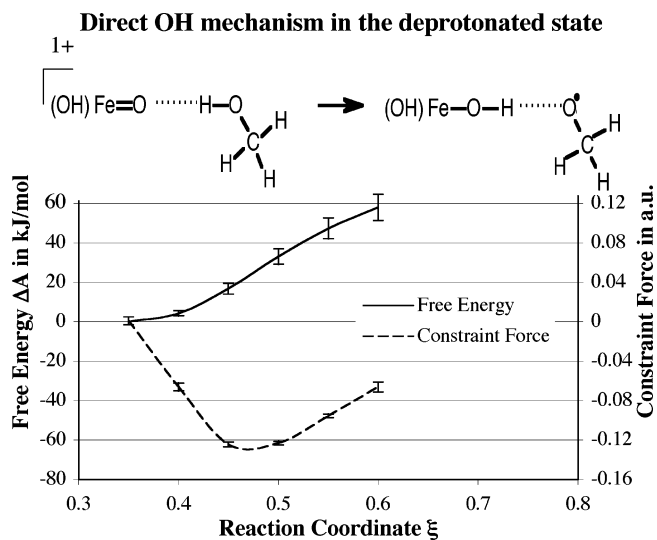


**Figure 13.** Thermodynamic integration results for the first step of the direct OH mechanism in the deprotonated state. The intermediate product is very unstable and makes it impossible to complete the series. The error bars in the free energy curve are based on the hysteresis in the ordinary protonated state and are only indicative.

to 202 kJ/mol, so the direct CH mechanism is completely inhibited when a water molecule in the first shell of the iron ion is deprotonated.

For the coordination OH mechanism, deprotonation of the complex is also disadvantageous for the reaction. As mentioned above, the deprotonated species we consider is the one in which the coordinated methanol has lost a proton. In this case the second step of the reaction consists of transfer of a methyl H to the oxido oxygen. We calculated a barrier of 87 kJ/mol for this second step (vs 38 kJ/mol before).

Apparently, for all mechanisms, a relatively high pH (relative to  $pK_a = 2$ ), at which deprotonated states start to become abundant, is disadvantageous for the reaction. This fits in with the fact that the Fenton reaction is optimally performed in acidic solution,  $pH = 3-5$ . Too high pH would of course be problematic anyway, since ironhydroxide complexes are not soluble in basic solutions.

**(b) Solution.** For completeness, we also performed one series of Car-Parrinello simulations in solution with the deprotonated reactant (conjugate base)  $[\text{FeO}(\text{H}_2\text{O})_4\text{OH}]^+$ . These simulations were performed for the direct OH mechanism. In this case, the reactants complex was stable during a test simulation of 15 ps, in contrast to what we found before for the complexation to  $[\text{FeO}(\text{H}_2\text{O})_5]^{2+}$ . With the conjugate base, a stable hydrogen bond is formed with the oxido oxygen as H-bond acceptor (electron donor), which is, apparently, much less influenced by the solvent than the charge transfer interaction in the normal case.

The results of the thermodynamic integration are shown in Figure 13. The intermediate product turns out to be even more unstable in the deprotonated state than it was in the protonated state. As a consequence, in all simulations beyond  $\xi = 0.6$ , the molecules react back to the reactants via a chain mechanism. In these simulations, a hydrogen atom of one of the ligands (either a water ligand or an  $\text{OH}^-$  ligand) is transferred to the  $\text{CH}_3\text{O}^\bullet$  radical via solvent water molecules, resulting in reformation of the reactants. The simulations beyond  $\xi = 0.6$  could thus not be performed and the series could not be completed. Nevertheless, the trend is clear: in a relatively basic solution  $\text{FeO}^{2+}$  is even less likely to abstract the OH hydrogen for the direct OH mechanism than in an acidic solution.

In conclusion, we find that deprotonation weakens the reactivity of  $[\text{FeO}(\text{H}_2\text{O})_5]^{2+}$  for the direct CH and OH mechanisms, and also for the coordination OH mechanism. Especially for the direct mechanisms the effect of deprotonation has a similar electronic origin as the effect of solvation. Deprotonation changes the overall charge from +2 to +1. This causes a relative upshift of the LUMO, which strongly diminishes the peculiarly strong charge transfer interaction of the very low-lying  $\text{FeO}^{2+}$  LUMO with the organic substrate. Long-range dielectric screening effects of the solvent have the same effect: the charge transfer interaction is weakened because the LUMO of  $\text{FeO}^{2+}$  is shifted upward more than the orbital levels of the neutral organic substrate. The effect of deprotonation is less striking in solution, because, once the charge transfer interaction is weakened, another upshift of the LUMO has much less effect.

## 6. Conclusion

We have studied the mechanism of the oxidation of methanol by  $\text{FeO}^{2+}$  in water, as a prototype for alcohol oxidation in the Fenton chemistry. We find the direct CH mechanism to have the highest probability. In this mechanism, the methanol molecule first forms a complex bond with the oxido group with a methyl C–H bond in an approximately linear configuration to the Fe–O bond. The C–H bond is then attacked as the first step. In the gas-phase this mechanism has a spectacularly low barrier of only 2 kJ/mol (and the second step, the transfer of the OH hydrogen, even occurs without barrier). In solution the Helmholtz free energy barrier has been estimated to have an upper bound of 50 kJ/mol; the second step still occurs spontaneously. The first step of methanol oxidation via the direct CH mechanism is similar to the one in methane oxidation, where in this case an OH ligand and a weakly bound  $^\bullet\text{CH}_2\text{OH}$  radical are formed, but the second step is not the “rebound mechanism” of OH binding to the  $^\bullet\text{CH}_2\text{OH}$  radical, to form a di-alcohol. Instead, the H of the hydroxyl group of methanol is transferred without barrier to the OH ligand to form an  $\text{H}_2\text{O}$  ligand. This H transfer occurs through the solvent via a Grotthuss diffusion mechanism.

The high reactivity of the ironoxido complex toward aliphatic bonds like the methanol C–H bonds can be explained by the very low-lying  $\alpha$ -LUMO of  $\text{FeO}^{2+}$ , which is the Fe–O  $3\sigma^*$  orbital. This orbital reaches spatially beyond the occupied orbitals and makes the ironoxido ion very open to reaction at the oxido site. As a result,  $\text{FeO}^{2+}$  is a very strong electron acceptor, rather than being a hydrogen bond acceptor (in which case it would have to act as electron donor): a molecule that comes close enough to form a hydrogen bond starts to interact with the LUMO and forms a strong charge-transfer bond instead. The charge transfer from the C–H bonding orbital into the  $3\sigma^*$  activates the C–H bond. The charge transfer increases when the C–H bond is stretched, which compensates for the strain energy and lowers the barrier even more, enabling easy abstraction of a hydrogen atom.

We have observed that the solvent effects on the barriers of the direct mechanisms are very large (50 kJ/mol in water solvent vs 2 kJ/mol in the gas phase for the direct CH mechanism). A similar large increase in the barrier was observed in the methane to methanol oxidation by aqueous  $\text{FeO}^{2+}$  (from 14 kJ/mol to 92 kJ/mol).<sup>27</sup> We stress that this is not a display of a systematic problem in the microsolvated gas-phase calculations, but it is caused by a very specific solvation effect. When the system is brought into solution, the orbitals of the positively charged  $\text{FeO}^{2+}$  shift upward relative to those of the neutral methanol due to the screening of the solvent, and as a result, the charge

transfer interaction with the low-lying 3 $\sigma^*$  LUMO weakens. In turn, the activation of the methanol bonds is less pronounced and the reaction barriers increase.

Among the other mechanisms of Figure 1, we have been able to rule out the direct OH mechanism and the coordination CH mechanism. However, the coordination OH mechanism cannot be ruled out. Although the gas-phase barrier for hydrogen transfer from the OH group of coordinated methanol to the oxido oxygen is over 100 kJ/mol, the introduction of a bridging water molecule lowers the gas-phase barrier to 31 kJ/mol. The second step of H abstraction from the CH<sub>3</sub> group has a barrier of 38 kJ/mol.

In solution the easy hydrolysis of the coordinated methanol plays a role. Because of the high acidity of the Fe<sup>IV</sup> complexes, we envisage easy transfer of the hydroxyl H to the FeO<sup>2+</sup>, possibly along a chain of water molecules. The Helmholtz free energy barrier of the second step becomes 44  $\pm$  10 kJ/mol and is close to the energy barrier of 38 kJ/mol in the gas phase. This barrier makes the coordination OH mechanism competitive with the direct CH mechanism with its free energy barrier of 50 kJ/mol (upper bound). However, it should be kept in mind, that the coordination OH mechanism can only become operative after a water/methanol ligand substitution.

Because [FeO(H<sub>2</sub>O)<sub>5</sub>]<sup>2+</sup> is rather acidic (pK<sub>a</sub> = 2), it could very well be deprotonated, and therefore we also studied the reactivity of its conjugate base: [FeO(H<sub>2</sub>O)<sub>4</sub>OH]<sup>+</sup>. However, for all of the mechanisms of Figure 1, the reaction barriers become higher upon deprotonation. Clearly, the conjugate base of [FeO(H<sub>2</sub>O)<sub>5</sub>]<sup>2+</sup> is much less reactive, and relatively basic conditions will slow down the reaction. This relates well to the fact that a low pH is needed for the Fenton reaction (optimal pH 3–5). Of course, too high pH would hamper the reaction anyway due to precipitation of iron hydroxides.

The decreased reactivity of the conjugate base of [FeO(H<sub>2</sub>O)<sub>5</sub>]<sup>2+</sup>, especially for the direct mechanisms, has the same cause as the increase of the barriers in solution compared to the gas phase: the deprotonation makes the orbitals shift upward in energy, and as a result, the reactivity decreases. Finally, this also explains why in the deprotonated case the solvent effect is much smaller: The screening effects are smaller due to the smaller charge (+1 instead of +2), and the 3 $\sigma^*$  orbital is already shifted upward due to the lowering of the positive charge, diminishing the charge transfer interaction.

Electronic structure aspects of these reactions, including the importance of the 3 $\sigma^*$  LUMO for the reactivity of FeO<sup>2+</sup> and the explanation of the effect of solvation and of changes in the ligand environment, are the subject of separate investigations.<sup>47,71</sup>

**Acknowledgment.** We acknowledge the support from The Netherlands' National Research School Combination "Catalysis by Design" (NRSC-C). We thank the foundation NCF of The Netherlands' Foundation of Scientific Research (NWO) for computer time.

## References and Notes

- (1) Fenton, H. J. H. *Chem. News* **1876**, 190.
- (2) Bishop, D. F.; Stern, G.; Fleischman, M.; Marshall, L. S. *Ind. Eng. Chem. Des. Dev.* **1968**, *7*, 110–117.
- (3) Hage, J. P.; Llobet, A.; Sawyer, D. T. *Bioorganic Med. Chem.* **1995**, *3*, 1383.
- (4) Wardman, P.; Candeias, L. P. *Rad. Research* **1996**, *145*, 523–531.
- (5) Dunford, H. B. *Coord. Chem. Rev.* **2002**, *233*, 311–318.
- (6) Rush, J. D.; Koppenol, W. H. *J. Am. Chem. Soc.* **1988**, *110*, 4957–4963.
- (7) Koppenol, W. H. *Redox Rep.* **2001**, *6*, 229–234.
- (8) Groves, J. T. *J. Inorg. Biochem.* **2006**, *100*, 434–447.
- (9) Bray, W. C.; Gorin, M. H. *J. Am. Chem. Soc.* **1932**, *54*, 2124–2125.
- (10) Buda, F.; Ensing, B.; Gribnau, M. C. M.; Baerends, E. J. *Chem. Eur. J.* **2001**, *7*, 2775–2783.
- (11) Ensing, B.; Buda, F.; Blöchl, P.; Baerends, E. J. *Angew. Chem., Int. Ed. Engl.* **2001**, *40*, 2893–2895.
- (12) Ensing, B.; Buda, F.; Blöchl, P. E.; Baerends, E. J. *Phys. Chem. Chem. Phys.* **2002**, *4*, 3619–3627.
- (13) Ensing, B.; Baerends, E. J. *J. Phys. Chem. A* **2002**, *106*, 7902–7910.
- (14) Meunier, B.; de Visser, S. P.; Shaik, S. *Chem. Rev.* **2004**, *104*, 3947–3980.
- (15) Costas, M.; Chen, K.; Que, L. *Coord. Chem. Rev.* **2000**, *200–202*, 517–544.
- (16) Solomon, E. I.; Decker, A.; Lehnert, N. *Proc. Natl. Acad. Sci. U.S.A.* **2003**, *100*, 3589–3594.
- (17) Que, L. *J. Biol. Inorg. Chem.* **2004**, *9*, 684–690.
- (18) Schöneboom, J. C.; Cohen, S.; Lin, H.; Shaik, S.; Thiel, W. *J. Am. Chem. Soc.* **2004**, *126*, 4017–4034.
- (19) Groenhof, A. R.; Swart, M.; Ehlers, A. W.; Lammertsma, K. J. *Phys. Chem. A* **2005**, *109*, 3411–3417.
- (20) Bassan, A.; Blomberg, M. R. A.; Borowski, T.; Siegbahn, P. E. M. *J. Inorg. Biochem.* **2006**, *100*, 727–743.
- (21) Bassan, A.; Blomberg, M. R. A.; Siegbahn, P. E. M. *Chem. Eur. J.* **2003**, *9*, 4055–4067.
- (22) Kaizer, J.; Klinker, E. J.; Oh, N. Y.; Rohde, J. U.; Song, W. J.; Stubna, A.; Kim, J.; Munck, E.; Nam, W.; Que, L. *J. Am. Chem. Soc.* **2004**, *126*, 472–473.
- (23) van den Berg, T. A.; de Boer, J. W.; Browne, W. R.; Roelfes, G.; Feringa, B. L. *J. Chem. Soc., Chem. Commun.* **2004**, *22*, 2550–2551.
- (24) Rohde, J. U.; Que, L. *Angew. Chem., Int. Ed.* **2005**, *44*, 2255–2258.
- (25) Pestovsky, O.; Stoian, S.; Bominaar, E. L.; Shan, X.; Munck, E.; Que, L.; Bakac, A. *Angew. Chem., Int. Ed.* **2005**, *44*, 6871–6874.
- (26) Kremer, M. L. *Int. J. Chem. Kinet.* **2006**, *38*, 725–736.
- (27) Ensing, B.; Buda, F.; Gribnau, M. C. M.; Baerends, E. J. *J. Am. Chem. Soc.* **2004**, *126*, 4355–4365.
- (28) Groves, J. T.; McClusky, G. A. *J. Am. Chem. Soc.* **1976**, *98*, 859–861.
- (29) Groves, J. T.; Van, Der, Puy, M. *J. Am. Chem. Soc.* **1976**, *98*, 5290–5297.
- (30) <http://www.h2o2.com/applications/industrialwastewater/hcho.html> and <http://www.h2o2.com/applications/industrialwastewater/fentonsreagent.html>.
- (31) Shiota, Y.; Yoshizawa, K. *J. Am. Chem. Soc.* **2000**, *122*, 12317–12326.
- (32) Yumura, T.; Yoshizawa, K. *Organometallics* **2001**, *20*, 1397–1407.
- (33) Yoshizawa, K.; Kagawa, Y. *J. Phys. Chem. A* **2000**, *104*, 9347–9355.
- (34) Fiedler, A.; Schröder, D.; Shaik, S.; Schwarz, H. *J. Am. Chem. Soc.* **1994**, *116*, 10734–10741.
- (35) Schröder, D.; Schwarz, H.; Shaik, S. In *Structure & Bonding: Metal-oxo and metal-peroxo species in catalytic oxidations*; Meunier, B., Ed.; Springer-Verlag: Berlin, 2000; Vol. 97, pp 91–123.
- (36) Schröder, D.; Shaik, S.; Schwarz, H. *Acc. Chem. Res.* **2000**, *33*, 139–145.
- (37) Harris, N.; Shaik, S.; Schröder, D.; Schwarz, H. *Helv. Chim. Acta* **1999**, *82*, 1784–1797.
- (38) Buda, F.; Ensing, B.; Gribnau, M. C. M.; Baerends, E. J. *Chem. Eur. J.* **2003**, *9*, 3436–3444.
- (39) Decker, A.; Solomon, E. I. *Curr. Opin. Chem. Biol.* **2005**, *9*, 152–163.
- (40) Decker, A.; Rohde, J. U.; Que, L.; Solomon, E. I. *J. Am. Chem. Soc.* **2004**, *126*, 5378–5379.
- (41) Kumar, D.; Hirao, H.; Que, L.; Shaik, S. *J. Am. Chem. Soc.* **2005**, *127*, 8026–8027.
- (42) Decker, A.; Solomon, E. I. *Angew. Chem., Int. Ed.* **2005**, *44*, 2252–2255.
- (43) Decker, A.; Clay, M. D.; Solomon, E. I. *J. Inorg. Biochem.* **2006**, *100*, 697–706.
- (44) Ghosh, A.; Tangen, E.; Ryeng, H.; Taylor, P. R. *Eur. J. Inorg. Chem.* **2004**, *2004*, 4555–4560.
- (45) Neese, F. *J. Inorg. Biochem.* **2006**, *100*, 716–726.
- (46) Jacobsen, F.; Holeman, J.; Sehested, K. *Int. J. Chem. Kinet.* **1998**, *30*, 215–221.
- (47) Louwse, M. J.; Baerends, E. J. *Phys. Chem. Chem. Phys.* **2007**, *9*, 156–166.
- (48) Becke, A. *Phys. Rev. A* **1988**, *38*, 3098.
- (49) Lee, C.; Yang, W.; Parr, R. G. *Phys. Rev. B* **1988**, *37*, 785.
- (50) Sprik, M.; Hutter, J.; Parrinello, M. *J. Chem. Phys.* **1996**, *105*, 1142.
- (51) de Jong, G. T.; Geerke, D. P.; Diefenbach, A.; Bickelhaupt, F. M. *Chem. Phys.* **2005**, *313*, 261–270.

- (52) Swart, M.; Groenhof, A. R.; Ehlers, A. W.; Lammertsma, K. *J. Phys. Chem. A* **2004**, *108*, 5479–5483.
- (53) Fouqueau, A.; Mer, S.; Casida, M. E.; Daku, L. M. L.; Hauser, A.; Mineva, T.; Neese, F. *J. Chem. Phys.* **2004**, *120*, 9473–9486.
- (54) Amsterdam Density Functional program, Theoretical Chemistry, Vrije Universiteit, Amsterdam, URL: <http://www.scm.com>.
- (55) Baerends, E. J.; Ellis, D. E.; Ros, P. *Chem. Phys.* **1973**, *2*, 41.
- (56) Fonseca, Guerra, C.; Snijders, J. G.; te Velde, G.; Baerends, E. J. *Theor. Chem. Acc.* **1998**, *99*, 391.
- (57) te Velde, G.; Bickelhaupt, F. M.; van Gisbergen, S. J. A.; Fonseca, Guerra, C.; Baerends, E. J.; Snijders, J. G.; T., Z. *J. Comput. Chem.* **2001**, *22*, 931.
- (58) van Lenthe, E.; Baerends, E. J.; Snijders, J. G. *J. Chem. Phys.* **1994**, *101*, 9783.
- (59) Blöchl, P. *Phys. Rev. B* **1994**, *24*, 17953.
- (60) Vassilev, P.; Louwerse, M. J.; Baerends, E. J. *Chem. Phys. Lett.* **2004**, *398*, 212–216.
- (61) Vassilev, P.; Louwerse, M. J.; Baerends, E. J. *J. Phys. Chem. B* **2005**, *109*, 23605–23610.
- (62) Frenkel, D.; Smit, B. *Understanding Molecular Simulation*; Academic Press: San Diego, CA, 1996.
- (63) Ensing, B.; Meijer, E. J.; Blöchl, P. E.; Baerends, E. J. *J. Phys. Chem. A* **2001**, *105*, 3300–3310.
- (64) Sprik, M.; Ciccotti, G. *J. Chem. Phys.* **1998**, *109*, 7737–7744.
- (65) den Otter, W. K.; Briels, W. J. *J. Chem. Phys.* **1998**, *109*, 4139–4146.
- (66) Flyvbjerg, H.; Petersen, H. G. *J. Chem. Phys.* **1989**, *91*, 461–466.
- (67) Mulliken, R. S. *J. Chem. Phys.* **1955**, *23*, 1833–1840.
- (68) Hirshfeld, F. L. *Theoret. Chim. Act.* **1977**, *44*, 129.
- (69) Bickelhaupt, F. M.; van Eikema Hommes, N. J. R.; Fonseca, Guerra, C.; Baerends, E. J. *Organometallics* **1996**, *15*, 2923–2931.
- (70) Newcomb, M.; Le Tadic-Biadatti, M. H.; Chestney, D. L.; Roberts, E. S.; Hollenberg, P. F. *J. Am. Chem. Soc.* **1995**, *117*, 12085–12091.
- (71) Bernasconi, L.; Louwerse, M. J.; Baerends, E. J. *Eur. J. Inorg. Chem.* **2007**, 3023–3033.